Thermochemistry of the HOSO Radical, a Key Intermediate in Fossil Fuel Combustion

Steven E. Wheeler* and Henry F. Schaefer III

Center for Computational Quantum Chemistry, University of Georgia, Athens, Georgia 30602

Received: March 31, 2009; Revised Manuscript Received: April 27, 2009

Despite the key role of the HOSO radical in the combustion of sulfur-rich fuels, the thermochemistry of this simple species is not well-established. Due to the extraordinary sensitivity of the potential energy surface to basis set and electron correlation methods in ab initio computations, there is no consensus in the literature regarding the structure of the global minimum *syn*-HOSO. A definitive enthalpy of formation for HOSO is presented, based on systematically extrapolated ab initio energies, accounting for electron correlation primarily through coupled cluster theory, including up to single, double, and triple excitations with a perturbative correction for connected quadruple excitations [CCSDT(Q)]. These extrapolated valence electronic energies have been corrected for core−electron correlation, harmonic and anharmonic zero-point vibrational energy, and non-Born−Oppenheimer and scalar relativistic effects. Our final recommended enthalpy of formation is $\Delta_f H_0°$(*syn*-HOSO) = −58.0 kcal mol^{-1}. The planar *anti*-HOSO transition state lies 2.28 kcal mol^{-1} above the *syn*-HOSO minimum, while predicted reaction enthalpies for H + SO_2 → HOSO, HOSO → OH + SO, HOSO + H → H_2 + SO_2, and OH + HOSO → SO_2 + H_2O are −38.6, 68.0, −64.4, and −80.1 kcal mol^{-1}, respectively. We provide incontrovertible evidence for a quasi-planar structure of the *syn*-HOSO radical, with a remarkably flat torsional energy surface, based on CCSD(T) geometries and harmonic vibrational frequencies energies with up to quintuple-ζ quality basis sets. The energy separation between planar *syn*-HOSO and the nonplanar global minimum is a mere 5 cm^{-1} at the cc-pV(T+D)Z CCSD(T) level of theory. Computed fundamental vibrational frequencies for *syn*-HOSO and *syn*-DOSO based on a full quartic force-field evaluated at the cc-pV(T+d)Z CCSD(T) level of theory are in agreement with available experimental data. The present results confirm a previously tentative assignment of a band at 1050 cm^{-1} to the HOS bending mode.

I. Introduction

There has been renewed interest in the combustion of sulfur-containing fuels,[1–4] due in part to increased efforts to reduce noxious emissions from the burning of fossil fuels. Sulfur is present in fossil fuels and despite its low concentration can have a significant impact on combustion.[5] During combustion, gaseous sulfur is primarily present as sulfur dioxide, which has profound effects on flame behavior[6–11] and explosion limits[12] due to the catalytic removal of chain propagating radical species.[7,10,12–18] Specifically, the presence of SO_2 inhibits CO oxidation through the catalytic removal of atomic oxygen and hydrogen and similarly affects NO_x chemistry in flames. The effect on NO_x chemistry occurs via direct interaction of SO_2 with nitrogen containing species and indirectly through the catalytic removal of chain carrying radicals.

The catalytic removal of H atoms by SO_2 in flames was traditionally described as occurring via reactions 1−3, though recent results[5,19] have indicated a more complex mechanism coupling these processes to additional reaction cycles involving HSO, SH, and S.

$$H + SO_2 + M \rightarrow HOSO + M \quad (1)$$

$$HOSO + H \rightarrow SO_2 + H_2 \quad (2)$$

$$HOSO + OH \rightarrow SO_2 + H_2O \quad (3)$$

Regardless, the rate-limiting step in the removal of atomic hydrogen is reaction 1 and enthalpy of formation for the HOSO radical, as well as the enthalpies of reactions 1−3, are key parameters in quantitative models of the combustion of sulfur-containing fuels.[2,13,17,18,20–25] Unfortunately, attempts to model such processes are often mired by uncertainties in the underlying thermochemistry.[13,24]

The HOSO radical was first identified in the gas phase in 1996 by Frank, Sadilek, Ferrier, and Tureček[26] using neutralization−reionization mass spectrometry. This was followed several years later by two rare-gas matrix isolation studies by Isoniemi, Khriachtchev, Lundell, and Räsänen,[27,28] in which infrared bands corresponding to three of the vibrational modes were assigned based on comparisons with harmonic frequencies computed using second- and forth-order Møller−Plesset perturbation theory (MP2 and MP4). A fourth transition at 1050 cm^{-1} was tentatively assigned to the HOS bending mode.[28]

Numerous detailed kinetic models have been developed for the oxidation of sulfur under combustion conditions.[2,13,17,18,20–25] These include the early work of Zachariah and Smith,[13] as well as more recent work based on ab initio computed potential energy surfaces and RRKM-derived rate constants.[17,18,20,21] Dagaut and co-workers[22–25] published a series of combined experimental and modeling studies examining the effects of SO_2 on NO_x chemistry and CO oxidation in flames, while Cerru,

* Corresponding author, swheele2@chem.ucla.edu.

10.1021/jp9029387 CCC: $40.75
Published on Web 05/21/2009

Kronenburg, and Lindstedt recently presented[2] a detailed mechanism for sulfur oxidation validated against experimental flame data. More recently, Blitz, Hughes, Pilling, and Robertson[3] examined the pressure and temperature dependence of predicted rate constants through a solution of the master equation for the multiwell reaction of H + SO_2, using relative energies and reaction barriers from the work of Frank et al.[29] and Goumri and co-workers.[30] However, these master equation results are potentially tainted by uncertainties in the underlying G2(MP2) computations, which rely exclusively on spin-unrestricted MP2 (MP2) paired with small basis sets for optimized geometries. As discussed below, MP2 yields spurious predictions for both geometries and energies for the HOSO radical when paired with many popular basis sets. Indeed, all previous modeling studies have relied on tenuous theoretical predictions of thermochemical parameters and rate constants for reactions associated with the HOSO radical.

There have been numerous theoretical investigations of the HOSO radical and associated reactions over the last three decades,[26,29–43] spanning the gamut of ab initio and DFT methods. Initially, the consensus was that the global minimum configuration adopts a planar *syn*-HOSO structure, while the corresponding planar *anti* rotamer is a transition state. The first theoretical study of Boyd, Gupta, Langler, Lownie, and Pincock[31] included optimized geometries and harmonic vibrational frequencies of HOSO and related radicals, computed using unrestricted Hartree−Fock theory with a small basis set. A series of papers was subsequently published in the 1990s by Marshall and co-workers,[30,32,33] detailing thermochemical investigations of the HOSO radical and the potential energy surfaces for the H + SO_2 and HS + O_2 reactions. Among other data, this work included an enthalpy of formation for *syn*-HOSO radical of −56.7 kcal mol^{-1}, computed via the atomization energy using a G2-like approach.[33] Morris and Jackson[34] presented geometries and harmonic vibrational frequencies (as well as potential energy surfaces for H + SO_2) using UMP2 with a DZP basis set, concluding that both *syn*- and *anti*-HOSO are minima on the potential energy surface, in contrast to previous correlated computations.[30,32,33] Meanwhile, Frank et al.[26,29] presented two joint experimental/theoretical studies including G2(MP2) potential energy surfaces for key HOSO reactions. Again, the UMP2 optimizations and harmonic vibrational frequencies utilized in the G2(MP2) approach indicated that both *syn*- and *anti*-HOSO are local minima.

In 1998, Drozdova and co-workers reported[36] an ab initio study of $H_xS_yO_z$ (x, y, z = 0−2), including ANO UCCSD(T) energies computed at 6-311+G(d,p) UMP2 geometries for the planar *syn*-HOSO radical. Three years later, McKee and Wine[37] published 6-31+G(d) B3LYP geometries and vibrational frequencies, indicating that at this level of theory, both *syn*- and *anti*-HOSO configurations are *transition states*, not minima. Instead, 6-31+G(d) B3LYP computations place a staggered HOSO radical as the global minimum, in contrast to previous ab initio results. Shortly thereafter, Wang and Zhang published[38] enthalpies of formation of *syn*-HOSO, *anti*-HOSO, and a staggered HOSO configuration computed via atomization reactions using the G3B3 and G3 methods. Wang and Hou presented[39] a nonplanar *syn*-HOSO geometry computed at the aug-cc-pV(T+d)Z B3LYP level of theory.

In 2005, Ballester and Varandas[41] published a double many-body expansion (DMBE) of the HOSO potential, parametrized in part against complete active space SCF (CASSCF) geometries and vibrational frequencies computed with DZ and TZ basis sets. While the CASSCF computations predict a planar *syn*-HOSO configuration, the DMBE potential yields a staggered global minimum structure. This global DMBE potential energy surface was used in a subsequent quasi-classical trajectory study[42] of the OH + SO → H + SO_2 reaction, revealing that this reaction proceeds via a single intermediate, namely, the HOSO radical. A more recent study[40] by Napolion and Watts set to resolve the quandary of the planarity of the *syn*- and *anti*-HOSO geometries through coupled cluster computations. Unfortunately, the question remained unanswered due to the encountered basis set sensitivity of the torsional potential energy surface: 6-31+G(d) UCCSD(T) and 6-311G(d,p) UCCSD(T) computations predict that both the *syn*- and *anti*-HOSO are transition states, while cc-pVTZ UCCSD(T) optimizations and frequencies predict a planar *syn*-HOSO global minimum with the *anti* rotamer a first-order saddle point on the PES. Wierzejewska and Olbert-Majkut published[43] restricted and unrestricted MP2 results, predicting a nonplanar *syn*-HOSO minimum with a restricted open-shell formalism and a planar *syn* structure with UMP2, both using a 6-311++G(2d,2p) basis.

Despite the small size of the seemingly simple HOSO radical, we see that results from previous theoretical studies[26,29–44] are remarkably inconsistent. While many previous results support a planar *syn*-HOSO configuration as the global minimum with the *anti* rotamer a first-order saddle point, the body of theoretical results is unsatisfactorily inconsistent in this regard. These inconsistencies arise primarily from an uncanny sensitivity of the HOSO potential energy surface to both basis set and electron correlation method, leading to myriad predictions of both planar and nonplanar global minimum geometries. Accompanying this confusion surrounding the geometry is a similarly unsatisfactory dearth of accurate thermochemical data for HOSO, with predicted enthalpies of formation for HOSO spanning a stunning 16 kcal mol^{-1}.[2,24,32,38,45]

Given the importance of the HOSO radical in the combustion of sulfur-containing fuels (i.e., fossil fuels), and the implications for NO_x chemistry and the oxidation of CO in flames, accurate theoretical treatments of the thermochemistry of reactions 1−3 and a precise determination of $\Delta_f H_0°$ for the HOSO radical are long overdue. Definitive thermochemical determinations are presented, achieved through systematic extrapolations of ab initio energies, corrected for core-correlation, scalar relativistic, and non-Born−Oppenheimer effects as well as harmonic and anharmonic zero-point vibrational energies. The basis set sensitivity of the HOSO potential energy surface is combated through the use of large modern basis sets,[46] which ameliorate many of the issues encountered in previous work, combined with extrapolations to the complete basis set limit.

We proceed by first describing our theoretical approach (section II), followed by a discussion of optimized structures for *syn*- and *anti*-HOSO (section III) and a thorough examination of the problematic torsional potential energy surface of the HOSO radical in section IV. In section V we analyze predicted vibrational frequencies for the global minimum *syn*-HOSO radical, while in section VI the enthalpy of formation of *syn*- and *anti*-HOSO as well as the enthalpies of key reactions are presented. Results are summarized in section VII.

II. Theoretical Methods

Precise relative energies of stationary points on the HOSO torsional potential energy surface have been computed using the focal point analysis (FPA) method of Allen and co-workers.[47–50] The focal point paradigm provides a framework within which one executes dual one- and n-particle expansions, extrapolating to the complete basis set limit (CBS) using the correlation-

TABLE 1: Reference Enthalpies of Formation (kcal mol^{-1})[a]

species	$\Delta_f H_{0K}°$	$\Delta_f H_{298K}°$	uncertainty
H	51.63	52.10	0.00
OH	8.86	8.93	0.01
SO	0.99	0.99	0.04
SO_2	–70.75	–71.35	0.04
H_2O	–57.10	–57.80	0.01

[a] From the Active Thermochemical Tables (ATcT).[77–81]

consistent polarized valence hierarchy (cc-pV*X*Z) developed by Dunning. For sulfur, the standard cc-pV*X*Z basis sets[51,52] have been shown to yield anomalous predictions when extrapolating to the CBS limit,[53–56] prompting the introduction of the cc-pV(*X*+d)Z and aug-cc-pV(*X*+d)Z basis sets in 2001.[46] The latter basis sets were used in the focal point procedure. Electron correlation is treated through second-order perturbation theory, and primarily by coupled cluster theory including single and double excitations (CCSD)[57–60] and a perturbative treatment of triple excitations [CCSD(T)],[61–64] as well as CCSDT[65–68] with a perturbative correction for quadruple excitations [CCSDT-(Q)].[69,70] The CCSDT(Q) method was recently implemented by Bomble, Stanton, Kállay, and Gauss,[69] derived from a non-Hermitian perturbation theory analogous to that used to justify[71] the venerable (T) approximation for connected triple excitations.[72] CCSDT(Q) computations were done using MRCC[73,74] paired with the Mainz−Austin−Budapest version of ACES II.[75] Molpro[76] was used to evaluate the other energies required for the focal point analyses.

The enthalpy of formation of the HOSO radical was determined using the focal-point approach[47–50] applied to reactions 4 and 5. Enthalpies of formation for the reference compounds (H, SO_2, OH, and SO) are provided in Table 1 taken from the Active Thermochemical Tables (ATcT) of Ruscic and co-workers.[77–81]

$$H + SO_2 \rightarrow \textit{syn}\text{-HOSO} \quad (4)$$

$$\textit{syn}\text{-HOSO} \rightarrow OH(^2\Pi) + SO(^3\Sigma^-) \quad (5)$$

ROHF-based coupled cluster methods were used, denoted by ROCCSD and ROCCSD(T).[82] The second-order perturbative contribution to the valence focal point energies was similarly derived from restricted Møller−Plesset theory (RMP2).[83,84] The CCSDT(Q) method[69] is not yet implemented for ROHF reference wave functions, so corrections to the ROCCSD(T) energies for connected quadruple excitations were estimated by the difference between spin-unrestricted UCCSDT(Q) and UCCSD(T) computations. Since high-order coupled-cluster wave functions are only very weakly dependent on reference orbitals, the use of an unrestricted formalism is expected to have negligible effects, even in the presence of spin-contamination. All correlated energy computations involved the freezing of the carbon 1s orbitals, except for relativistic corrections and where noted otherwise for the evaluation of the core-correlation contribution. Hartree−Fock energies were extrapolated using a standard exponential form[85]

$$E_{HF} = a + be^{-cX} \quad (6)$$

while the correlation energies were extrapolated via[86]

$$E_{corr} = a + bX^{-3} \quad (7)$$

Core−electron correlation corrections were computed as the difference between all-electron and frozen-core cc-pCVTZ ROCCSD(T) energies. Non-Born−Oppenhiemer effects were accounted for via the diagonal Born−Oppenheimer correction (DBOC),[87–91] which constitutes the first-order perturbative correction to the Born−Oppenheimer energy, at the aug-cc-pV(T+d)Z ROHF level of theory using the Mainz−Austin−Budapest version of ACES II.[75] Similarly, special relativity was accounted for by the application of standard perturbation formulas for the mass-velocity and one-electron Darwin scalar relativistic effects,[92–96] computed at the all-electron cc-pCVTZ ROCCSD(T) level of theory[97] using ACES II.[98] A first-order spin−orbit correction of -38.2 cm^{-1} was applied to the energy of OH.[78] All computations required for the focal point method were executed at cc-pV(5+d)Z CCSD(T) optimized geometries.

To examine the dependence of the torsional bending frequency of the *syn*- and *anti*-HOSO radicals on level of theory, we have optimized these two stationary points using the cc-pV*X*Z (*X* = D, T, Q, 5), cc-pV(*X*+d)Z (*X* = D, T, Q, 5), aug-cc-pV*X*Z (*X* = D, T, Q), and aug-cc-pV(*X*+d)Z (*X* = D, T, Q) basis sets paired with ROHF, RMP2, ROCCSD, and ROCCSD(T), followed by the computation of the torsional harmonic vibrational frequency by finite differences of energies. Geometries and frequencies were also computed using cc-pVDZ ROCCSDT and cc-pV(D+d)Z ROCCSDT.

Anharmonic corrections to the cc-pV(5+d)Z ROCCSD(T) harmonic frequencies come from anharmonicity constants computed via second-order vibrational perturbation theory (VPT2)[99,100] applied to computed cubic and quartic force constants. The required force constants were computed in internal coordinates by finite differences of frozen-core cc-pV(T+d)Z ROCCSD(T) energies. The program INTDIF2005[101,102] was used to determine the necessary displaced geometries and force constants in internal coordinates. The transformation of the force constants from internal to normal coordinates was performed using INTDER2005[103–106] while spectroscopic constants were computed using ANHARM.[106,107] Due to the large amplitude motion associated with the torsional mode of *syn*-HOSO (ν_6), VPT2 cannot be utilized. Consequently, VPT2 was applied to the remaining vibrational modes, excluding the contribution from anharmonicity constants involving ν_6. The errors from neglecting these contributions to the fundamental frequencies are expected to be small (<5 cm^{-1}). The anharmonic contribution of ν_6 to the ZPVE was similarly neglected. Harmonic and anharmonic frequencies for *syn*-HOSO were evaluated at the planar stationary point. However, the perpendicular frequencies change only slightly along the torsional mode, and the effect on the predicted fundamental frequencies will be small.

III. Geometries

Optimized geometries for the planar *syn*- and *anti*-HOSO radical are included in Figure 1, computed using ROCCSD(T) paired with the cc-pVQZ, cc-pV5Z, cc-pV(Q+d)Z, and cc-pV(5+d)Z basis sets. With these large basis sets the geometries are well-converged; differences among the results are minor. Specifically, there is a slight shortening of the S−O bonds with increased basis set size accompanied by small increases in the HOS and OSO angles. Comparing the *syn*- and *anti*-periplanar geometries, there are minor changes in bond length upon rotation about the HOSO torsional angle. The central SO bond expands

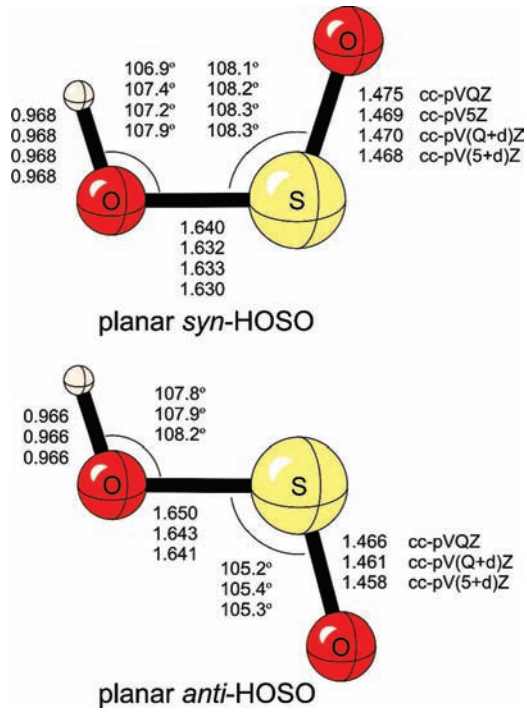

Figure 1. Optimized ROCCSD(T) geometries with the indicated basis sets for planar *syn*-HOSO and *anti*-HOSO. Distances are in angstroms and angles in degrees.

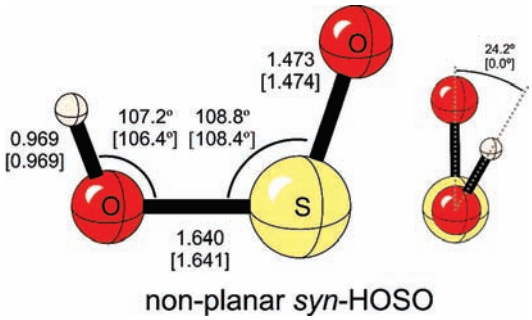

Figure 2. Optimized cc-pV(T+d)Z ROCCSD(T) geometry for nonplanar *syn*-HOSO. The cc-pV(T+d)Z ROCCSD(T) geometric parameters of the planar *syn*-HOSO radical are provided in brackets. Distances are in angstroms and angles in degrees.

by 0.01 Å while the terminal SO bond contracts an equal amount. The largest change is observed for the OSO angle, which shrinks by three degrees going from *syn*-HOSO to *anti*-HOSO. The HOS angle changes only slightly. In contrast to the observed sensitivity of the torsional potential energy surface (vide infra) the cc-pV*X*Z and cc-pV(*X*+d)Z basis sets yield similar geometries, with the exception of the HOS angle of *syn*-HOSO, which expands by 0.5° going from cc-pV5Z to cc-pV(5+d)Z.

As discussed below, the minimum energy *syn*-HOSO structure adopts a slightly nonplanar geometry, with a torsional angle of 24.2°. The cc-pV(T+d)Z ROCCSD(T) optimized nonplanar structure is provided in Figure 2. Bond distances and angles at the same level of theory for the planar *syn*-HOSO stationary point are listed in brackets for comparison. The geometry changes only slightly along this torsional coordinate, in accord with the small differences between the structures of planar *syn*- and *anti*-HOSO. The primary change is a decrease in the HOS and OSO angles of just under 1° in the former case and under 0.5° in the latter case.

IV. Torsional Potential Energy Surface

Previous theoretical work on the HOSO radical is inconsistent with regard to the nature of the torsional potential energy surface, with no consensus on the curvature at the planar *syn* and *anti* stationary points.[26,29–44] A panoply of torsional harmonic vibrational frequencies for planar *syn*- and *anti*-HOSO radicals are presented in Table 2 computed using the cc-pV*X*Z, cc-pV(*X*+d)Z, aug-cc-pV*X*Z, and aug-cc-pV(*X*+d)Z basis sets paired with ROHF, RMP2, ROCCSD, and ROCCSD(T) as well as ROCCSDT with the cc-pVDZ and cc-pV(D+d)Z basis sets. The effect of inclusion of core-correlation effects was also studied based on all electron cc-pCVDZ ROHF, RMP2, ROCCSD, and ROCCSD(T) computations. For the coupled-cluster results, the shifts due to additional tight basis functions and inclusion of core-correlation effects are minor, with the largest deviation of 9 cm^{-1} occurring for ROCCSD applied to *syn*-HOSO. RMP2 behaves less consistently, with the inclusion of core−electron correlation changing the torsional frequency of *anti*-HOSO by over 50 cm^{-1}.

The sensitivity to level of theory of the torsional energy surface surrounding the planar *syn*-HOSO radical is astounding, particularly for the standard cc-pVXZ and aug-cc-pVXZ basis sets. All methods paired with either the cc-pVDZ or aug-cc-pVDZ basis sets indicate that *syn*-HOSO is an energy minimum. Upon increase to a triple-ζ basis set, the curvature of the RMP2 surface at the *syn*-HOSO stationary point switches, indicated by the imaginary torsional frequency for cc-pVTZ RMP2 and aug-cc-pVTZ RMP2. With these correlation consistent basis sets up to quadruple-ζ quality, coupled cluster methods consistently predict *syn*-HOSO to be an energy minimum, though the curvature of the torsional surface at this stationary point decreases with increasing basis set size. With the cc-pVDZ basis set, the full inclusion of triple excitations (CCSDT) shifts the torsional frequency by about 10%, indicating the CCSD(T) approach is adequately recovering the effect of triple excitations. It is not until the cc-pV5Z basis set that coupled cluster theory predicts an imaginary torsional frequency for planar *syn*-HOSO.

The *anti*-HOSO radical shows a similar, though less pronounced, sensitivity to basis set and method. Again, RMP2 exhibits somewhat erratic behavior, predicting that *anti*-HOSO is a minimum when paired with either the cc-pVDZ or aug-cc-pVDZ basis sets but a transition state for larger basis sets. ROHF theory predicts that the *anti*-HOSO radical is an energy minimum, while coupled cluster theory consistently predicts an imaginary frequency for ν_6. Again, the difference between the CCSD(T) and CCSDT torsional frequency with a double-ζ basis set is small, and the CCSD(T) result should be well converged toward the full configuration interaction limit.

The cc-pV(*X*+d)Z and aug-cc-pV(*X*+d)Z basis sets[46] yield much more consistent behavior with respect to the curvature of the torsional energy surface of the HOSO radical. Specifically, while with the cc-pV*X*Z basis sets the qualitatively correct curvature at the planar *syn*-HOSO geometry was not attained until the very large cc-pV5Z basis set, with these new basis sets triple-ζ quality is sufficient. While previous work[53–56] has focused on errors in extrapolated cc-pV*X*Z energies for sulfur-containing species,[53–56] we see here a stark example of the standard cc-pV*X*Z basis sets providing exiguous predictions of qualitative features on the potential energy surface. For the *anti*-HOSO configuration the cc-pV*X*Z and cc-pV(*X*+d)Z basis sets yield very consistent results, and *anti*-HOSO is undoubtedly a

TABLE 2: Harmonic Vibrational Frequencies (cm^{-1}) for the Torsional Mode (ω_6) of the Planar *syn*- and *anti*-Rotamers of the HOSO Radical

basis set	ROHF	RMP2	ROCCSD	ROCCSD(T)	ROCCSDT
			syn-**HOSO**		
cc-pVDZ	109	206	104	135	119
cc-pVTZ	133	100*i*	61	72	
cc-pVQZ	125	118*i*	23	29	
cc-pV5Z	102	127*i*	52*i*	54*i*	
cc-pV(D+d)Z	69	55	50*i*	29	34
cc-pV(T+d)Z	98	135*i*	71*i*	68*i*	
cc-pV(Q+d)Z	107	134*i*	67*i*	68*i*	
cc-pV(5+d)Z	112	126*i*	57*i*	61*i*	
aug-cc-pVDZ	180	108	111	120	
aug-cc-pVTZ	148	102*i*	68	72	
aug-cc-pVQZ	133	105*i*	57	52	
aug-cc-pV(D+d)Z	154	106*i*	38	23	
aug-cc-pV(T+d)Z	117	128*i*	60*i*	61*i*	
aug-cc-pV(Q+d)Z	115	117*i*	40*i*	44*i*	
			anti-**HOSO**		
cc-pVDZ	192*i*	53	193*i*	172*i*	179*i*
cc-pVTZ	31	154*i*	125*i*	125*i*	
cc-pVQZ	83	150*i*	102*i*	106*i*	
cc-pV(D+d)Z	152*i*	116*i*	185*i*	175*i*	186*i*
cc-pV(T+d)Z	48	161*i*	127*i*	129*i*	
cc-pV(Q+d)Z	87	145*i*	102*i*	106*i*	
aug-cc-pVDZ	78	124	94*i*	73*i*	
aug-cc-pVTZ	93	129*i*	89*i*	85*i*	
aug-cc-pVQZ	100	123*i*	78*i*	78*i*	
aug-cc-pV(D+d)Z	119	108*i*	86*i*	88*i*	
aug-cc-pV(T+d)Z	108	128*i*	89*i*	91*i*	
aug-cc-pV(Q+d)Z	102	131*i*	77*i*	81*i*	

planar transition state corresponding to rotation about the H−O−S−O torsional angle.

To further explore the sensitivity of the MP2 torsional energy surface of the HOSO radical to basis set and address the inconsistencies in the literature,[26,29–44] relaxed energy curves along the H−O−S-O torsion angle (ϕ) are presented in Figures 3 and 4. In Figure 3, potential energy curves are given for RMP2 paired with the 6-31G(d), 6-31+G(d), cc-pVDZ, aug-cc-pVDZ, and cc-pVTZ basis sets, computed by performing constrained geometry optimizations for values of ϕ between 0 and 360° at 10° intervals. Unrestricted MP2 (UMP2) performs similarly. For comparison, a relaxed cc-pV(T+d)Z ROCCSD(T) curve is also included. The sensitivity of RMP2 is immediately apparent. Addition of diffuse functions to the basis set preferentially stabilizes the *anti*-HOSO rotamer for both 6-31G(d) and cc-pVDZ. RMP2 paired with cc-pVDZ incorrectly predicts *anti*-HOSO to be an energy minimum, as seen earlier in Table 2 and the addition of diffuse functions exacerbates this deficiency. Similarly, while 6-31G(d) RMP2 correctly predicts the curvature at $\phi = 180°$, the highly anharmonic shape of the potential at this point is not in accord with the CCSD(T) results. Inclusion of diffuse functions [6-31+G(d)] again lowers the energy of the *anti*-HOSO rotamer relative to surrounding configurations, yielding a remarkably flat potential between $\phi = 120$ and 240°. The cc-pVTZ basis set delivers a more adequate description of the potential surrounding $\phi = 180°$ but falters for ϕ near 0°. A close-up of the potential energy curves for $\phi = 0$ and 60° is provided in the bottom panel of Figure 2. RMP2 with the cc-pVTZ basis set correctly predicts the *syn*-HOSO radical to be a first-order saddle point but overestimates the extent of energy lowering upon breaking planarity. The smaller basis sets all predict a planar minimum and the curvatures of these surfaces at $\phi = 0°$ vary widely. The energies of *anti*-HOSO relative to the *syn*-rotamer predicted by RMP2 with these basis sets range from about 2.5 to almost 5 kcal mol^{-1}. Overall, MP2 is unsuited for the HOSO radical, exhibiting a profound sensitivity to basis set and yielding spurious predictions for geometries and relative energies of the *syn*- and *anti*-HOSO rotamers.

The cc-pV(D+d)Z and cc-pV(T+d)Z basis sets (see Figure 4) ameliorate many of these issues, correctly predicting the *syn*-HOSO radical to be a transition state when paired with RMP2. However, the curvature of the torsional potential at $\phi = 0$ still varies considerably, and cc-pV(T+d)Z RMP2 overestimates the energy lowering of the nonplanar *syn*-HOSO minimum slightly more than the cc-pVTZ basis set.

A focal point extrapolation[47–50] has been carried out in order to pinpoint the energy difference between *syn*- and *anti*-HOSO (Table 3). At the highest level for which explicit optimizations of the nonplanar *syn*-HOSO radical are currently practical [cc-pV(T+d)Z ROCCSD(T)], the energy lowering due to breaking planarity is less than 0.02 kcal mol^{-1}. As such, the focal point extrapolation was carried out using the planar *syn*- and *anti*-HOSO geometries. The effect of nonplanarity is simply subsumed into the error estimate in the final *syn*−*anti* energy difference of ±0.1 kcal mol^{-1}. The energy of *anti*-HOSO relative to *syn*-HOSO exhibits surprisingly little dependence on basis set, converging to an estimated valence complete basis set limit CCSDT(Q) value of 2.16 kcal mol^{-1}. Upon further corrections for core-correlation effects, harmonic zero-point vibrational energy, scalar relativistic effects, and non-Born−Oppenheimer effects, the final recommended energy of *anti*-HOSO relative to *syn*-HOSO is 2.28 ± 0.1 kcal mol^{-1}. This value is 0.5 kcal mol^{-1} higher than that reported by Frank et al.[29] based on the G2(MP2) model chemistry.

V. Fundamental Vibrational Frequencies

VPT2 has been applied to derive fundamental vibrational frequencies for *syn*-HOSO and the isotopologue *syn*-DOSO,

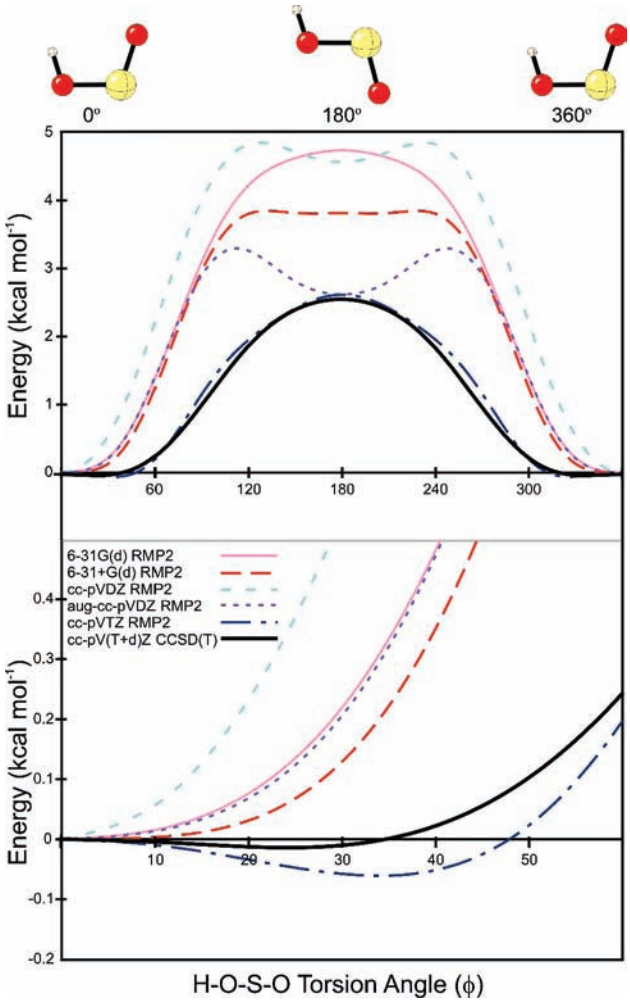

Figure 3. Relaxed energy scans along the H−O−S−O torsional angle ϕ at the 6-31G(d) RMP2, 6-31+G(d) RMP2, cc-pVDZ RMP2, aug-cc-pVDZ RMP2, cc-pVTZ RMP2, and cc-pV(T+d)Z ROCCSD(T) levels of theory.

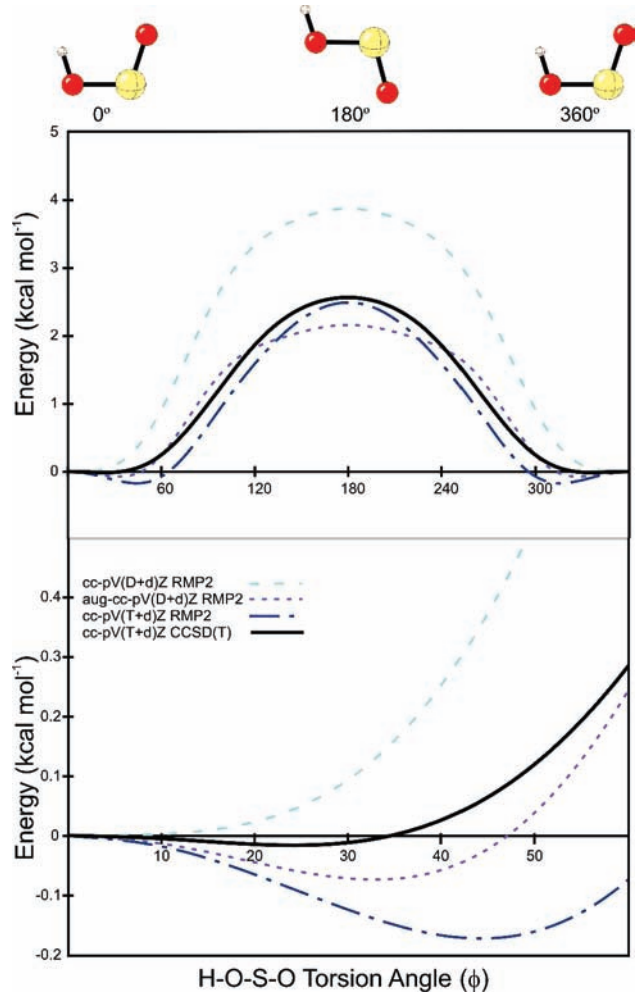

Figure 4. Relaxed energy scans along the H−O−S−O torsional angle ϕ at the cc-pV(D+d)Z RMP2, aug-cc-pV(D+d)Z RMP2, cc-pV(T+d)Z RMP2, and cc-pV(T+d)Z ROCCSD(T) levels of theory.

neglecting the coupling with the problematic torsional mode (ν_6). Results are presented in Table 4 Overall the agreement between the predicted fundamental frequencies and the results from the matrix isolation studies of Isoniemi and co-workers[27,28] is reasonable. IR data are available for *syn*-HOSO in Ar, Kr, and Xe matrices, providing a glimpse of the magnitude of matrix effects on the frequencies. Deviations between the present theoretical predictions and the experimental data decrease systematically going from Xe to Kr to Ar and the data suggest that our predicted values provide reliable estimates of the gas-phase fundamental frequencies. For each rare gas matrix, the largest deviation is for the OH stretch of HOSO (31, 51, and 71 cm^{-1} for the Ar, Kr, and Xe matrix results, respectively), in accord with expected magnitudes of matrix effects on different vibrational modes.[108] The predicted OD stretch in *syn*-DOSO is similarly 37 cm^{-1} larger than the experimental Kr value.[27] The other predicted fundamental frequencies are within about (15, 20, 25) cm^{-1} of the (Ar, Kr, Xe) experimental values. Isoniemi et al.[28] tentatively assigned the HOS stretch (ν_3) to 1050 cm^{-1}. The presently predicted ν_3 fundamental of 1055 cm^{-1} confirms this tentative assignment. Still more precise theoretical fundamental frequencies would be expected if the coupling to the highly anharmonic ν_6 were included.

VI. Enthalpy of Formation and Reaction Thermochemistry

The enthalpy of formation of the global minimum *syn*-HOSO radical has been computed using the focal point procedure of Allen and co-workers,[47–50] applied to reactions 4 and 5. Valence focal point tables for these reactions are provided in Table 5. Both reactions exhibit protracted convergence with respect to both basis set incompleteness and the inclusion of electron correlation. In reaction 4, the basis set dependence is largely recovered by the HF and MP2 contributions, with the aug-cc-pV(D+d)Z and CBS limit CCSD(T) increments differing by a mere 0.2 kcal mol^{-1}. In reaction 5, on the other hand, the double-ζ and CBS limit CCSD(T) increments differ by a more substantial 0.7 kcal mol^{-1}. Regardless, the final extrapolated CCSD(T) reaction energies are converged to well within 0.1 kcal mol^{-1} of the CBS limit in both cases. The slow convergence of the coupled cluster series is demonstrated by the CBS limit δROCCSD(T) increments of 2.4 and 3.3 kcal mol^{-1} for reactions 4 and 5, respectively. While these contributions are large, the CCSDT(Q) corrections are only 0.28 and 0.26 kcal mol^{-1}, suggesting that the final valence reaction energies are converged with respect to inclusion of electron correlation to our target accuracy of $\pm$0.2 kcal mol^{-1}. Correlation effects overall are significantly greater in the case of reaction 5, for which the HF

TABLE 3: Incremental Valence Focal Point Table (kcal mol^{-1}) for the Energy of *anti*-HOSO Relative to *syn*-HOSO[a]

basis set	ΔE_e[ROHF]	$+\delta$[RMP2]	$+\delta$[ROCCSD]	$+\delta$[ROCCSD(T)]	$=\Delta E_e$[ROCCSD(T)]
aug-cc-pV(D+d)Z	2.87	−0.77	+0.20	−0.07	[+2.22]
aug-cc-pV(T+d)Z	2.77	−0.73	+0.21	−0.09	[+2.17]
aug-cc-pV(Q+d)Z	2.75	−0.69	+0.22	−0.09	[+2.19]
aug-cc-pV(5+d)Z	2.75	−0.68	+0.22	−0.09	[+2.20]
aug-cc-pV(6+d)Z	2.74	−0.68	[+0.23]	[−0.09]	[+2.20]
CBS limit	[+2.74]	[−0.67]	[+0.23]	[−0.09]	[+2.21]

δ[UCCSDT(Q)/cc-pV(D+d)Z] = −0.05 kcal mol^{-1}; Final $\Delta E_{fp}(V) = 2.21 - 0.05 = 2.16$ kcal mol^{-1}

$E_0(\text{final}) = \Delta E_{fp}(V) + \Delta E_{core} + \Delta_{ZPVE} + \Delta_{rel} + \Delta_{DBOC}$

$= 2.16 + 0.02 + 0.07 + 0.03 + 0.00 =$ **2.28** kcal mol^{-1}

fit	$a + be^{-cX}$	$a + bX^{-3}$	$a + bX^{-3}$	$a + bX^{-3}$
points (X=)	4, 5, 6	5, 6	4, 5	4, 5

[a] The symbol δ denotes the increment in the energy difference (ΔE) with respect to the previous level of theory. Bracketed numbers are the result of basis set extrapolations (using the fits denoted in the table), while unbracketed numbers were explicitly computed. ΔE_{core} = core-correlation corrections at the cc-pCV(T+d)Z ROCCSD(T) level of theory; Δ_{ZPVE} = zero-point vibrational energy correction from cc-pV(5+d)Z ROCCSD(T) harmonic frequencies; Δ_{rel} = scalar relativistic corrections [cc-pCVTZ ROCCSD(T)]; ΔDBOC = diagonal Born−Oppenheimer correction [aug-cc-pV(T+d)Z ROHF].

TABLE 4: Predicted Harmonic (ω_i) and Fundamental Vibrational Frequencies (ν_i) for the *syn*-HOSO Radical and Deuterated *syn*-DOSO, Evaluated at the Planar Geometry[a]

		syn-HOSO					*syn*-DOSO		
	mode	ω_i	ν_i	exptl (Ar)	exptl (Kr)	exptl (Xe)	ω_i	ν_i	exptl (Kr)
ν_1	OH stretch	3757	3576	3544	3525	3504	2734	2639	2602
ν_2	SO stretch	1202	1184	1168	1164	1158	1190	1175	1160
ν_3	HOS bend	1085	1055		1050[c]		842	826	
ν_4	SO stretch	798	784	776	773	767	789	775	763
ν_5	OSO bend	392	389				368	365	

[a] Harmonic frequencies evaluated at the frozen-core cc-pV(5+d)Z ROCCSD(T) level of theory; anharmonic corrections from a frozen-core cc-pV(T+d)Z ROCCSD(T) full quartic force field. For comparison, experimental rare gas matrix isolation results are also included.[27,28] All values are in cm^{-1}. [b] Experimental fundamental vibrational frequencies are from matrix isolation studies in the indicated noble gas (ref 27). [c] Tentatively assigned in ref 28.

and final valence focal point energies differ by over 30 kcal mol^{-1}. The CBS limit MP2 results are in error by over 4 kcal mol^{-1} for both reactions 4 and 5, further demonstrating the unsuitability of MP2 for this system.

Upon inclusion of corrections for core-correlation, harmonic and anharmonic ZPVE, relativistic and non-Born−Oppenheimer effects, and spin−orbit coupling (for OH), the final 0 K enthalpies for reactions 4 and 5 are −38.64 and 68.03 kcal mol^{-1}, respectively. The former $\Delta_r H_0°$ value is 0.8 kcal mol^{-1} less exothermic than the G2(MP2) result of Frank et al.[29] (−39.4 kcal mol^{-1}) while the latter value is 1.1 kcal mol^{-1} smaller than Frank's suggested value of 69.1 kcal mol^{-1}.

Combining the enthalpies for reactions 4 and 5 with the reference enthalpies of formation for OH, SO, and SO_2 (Table 1), we arrive at $\Delta_f H_0°$(*syn*-HOSO) = −57.76 and −58.18 kcal mol^{-1}, respectively. The final recommended 0 K enthalpy of formation of the *syn*-HOSO radical is the average of these two values, −58.0 ± 0.4 kcal mol^{-1}. The corresponding 298 K value, in the rigid-rotor harmonic-oscillator approximation using cc-pV(T+d)Z CCSD(T) harmonic frequencies for the nonplanar *syn*-HOSO radical, is −58.8 ± 0.4 kcal mol^{-1}. Previously reported $\Delta_f H_0°$ values range from −44.7 to −60.9 kcal mol^{-1}.[2,24,32,38,45] The current recommendations are higher than the 0 K value of Marshall and co-workers[33] (−56.7 kcal mol^{-1}) and the 298 K values of Glarborg and co-workers[24] (−57.7 kcal mol^{-1}) and Wang and Zhang[38] (−57.1 kcal mol^{-1}).

The final recommended enthalpy of formation of HOSO can be combined with standard reference enthalpies for H, OH, SO_2, and H_2O from Table 1 to arrive at a recommended reaction enthalpy (0 K) for reactions 2 and 3 of −64.4 ± 0.4 and −80.1 ± 0.4 kcal mol^{-1}, respectively.

VII. Summary and Conclusions

The HOSO radical is central to combustion models of sulfur-containing fuels.[2,13,17,18,20–25] However, neither the enthalpy of formation nor thermochemistry of relevant reactions has been previously established. This is due in large part to the profound sensitivity to basis set in ab initio computations on the HOSO radical, which render many popular black-box approaches to computational thermochemistry less than satisfactory. This basis set sensitivity is particularly severe for the torsional energy surface.

The nonplanarity of the *syn* conformer has been conclusively established. HOSO adopts a quasi-planar structure with a broad, exceptionally flat torsional potential with a very small (5 cm^{-1}) barrier to planarity. The sensitivity of the torsional potential energy surface of HOSO has been studied at the MP2 level of theory, demonstrating the origin of previous discrepancies in the literature.[26,29–44] MP2 is unsuitable for application to the HOSO radical, casting doubt on results obtained using composite model chemistries that rely on MP2 for structures and energetics. It has also been shown that the standard cc-pV*X*Z and aug-cc-pVXZ basis sets yield a qualitatively incorrect potential energy surface when paired with ROCCSD(T) until basis sets of quintuple-ζ quality are reached. The cc-pV(X+d)Z and aug-cc-pV(X+d)Z basis sets[46] yield much more consistent results, providing a qualitatively correct ROCCSD(T) torsional PES already at the triple-ζ level. On the basis of systematically extrapolated ab initio energies, the recommended energy of the planar *anti*-HOSO transition state is 2.3 kcal mol^{-1}, relative to *syn*-HOSO.

TABLE 5: Incremental Valence Focal Point Table (kcal mol^{-1}) for Reactions 4 and 5[a]

basis set	ΔE_e[ROHF]	$+\delta$[RMP2]	$+\delta$[ROCCSD]	$+\delta$[ROCCSD(T)]	$= \Delta E_e$[ROCCSD(T)]
		$H + SO_2 \rightarrow$ *syn*-HOSO (4)			
aug-cc-pV(D+d)Z	−46.79	+2.88	−6.80	+2.19	[−48.53]
aug-cc-pV(T+d)Z	−41.71	+0.35	−6.84	+2.31	[−45.89]
aug-cc-pV(Q+d)Z	−41.25	+0.19	−6.72	+2.35	[−45.44]
aug-cc-pV(5+d)Z	−40.93	+0.29	−6.65	+2.37	[−44.93]
aug-cc-pV(6+d)Z	−40.80	+0.35	[−6.63]	[+2.37]	[−44.71]
CBS limit	[−40.75]	[+0.43]	[−6.61]	[+2.39]	[−44.54]
	δ[UCCSDT(Q)/cc-pVDZ] = +0.28 kcal mol^{-1}; $\Delta E_{fp}(V) = -45.54 + 0.28 = -44.26$ kcal mol^{-1}				
	ΔE_0(final) = $\Delta E_{fp}(V) + \Delta E_{core} + \Delta_{ZPVE} + \Delta_{anharm} + \Delta_{rel} + \Delta_{DBOC}$				
	$= -44.26 - 0.11 + 5.91 - 0.08 - 0.04 - 0.06 = \mathbf{-38.64}$ kcal mol^{-1}				
	$\Delta_f H_{0K}°(HOSO) = \mathbf{-57.76}$; $\Delta_f H_{298K}°(HOSO) = \mathbf{-58.62}$				
	syn-HOSO → OH($^2\Pi$) + SO($^3\Sigma^-$) (5)				
aug-cc-pV(D+d)Z	33.80	+28.52	−6.67	+2.57	[+58.22]
aug-cc-pV(T+d)Z	39.43	+32.27	−7.93	+3.06	[+66.83]
aug-cc-pV(Q+d)Z	40.02	+34.14	−7.87	+3.16	[+69.45]
aug-cc-pV(5+d)Z	40.17	+34.87	−7.94	+3.21	[+70.31]
aug-cc-pV(6+d)Z	40.25	+34.63	[−7.41]	[+3.23]	[+70.70]
CBS limit	[40.28]	[+34.29]	[−6.67]	[+3.26]	[+71.16]
	δ[UCCSDT(Q)/cc-pVDZ] = +0.26 kcal mol^{-1}; $\Delta E_{fp}(V) = 71.16 + 0.26 = 71.42$ kcal mol^{-1}				
	ΔE_0(final) = $\Delta E_{fp}(V) + \Delta E_{core} + \Delta_{ZPVE} + \Delta_{anharm} + \Delta_{rel} + \Delta_{DBOC} + \Delta_{SOSE}$				
	$= 71.42 + 0.25 - 3.33 + 0.04 - 0.31 + 0.06 - 0.11 = \mathbf{68.03}$ kcal mol^{-1}				
	$\Delta_f H_{0K}°(HOSO) = \mathbf{-58.18}$; $\Delta_f H_{298K}°(HOSO) = \mathbf{-59.00}$				
fit	$a + be^{-cX}$	$a + bX^{-3}$	$a + bX^{-3}$	$a + bX^{-3}$	
points (X=)	3, 4, 5	4, 5	3, 4	3, 4	

[a] The symbol δ denotes the increment in the energy difference (ΔE) with respect to the previous level of theory. Bracketed numbers are the result of basis set extrapolations (using the fits denoted in the table), while unbracketed numbers were explicitly computed. $\Delta E_{fp}(V)$ = valence focal point energy difference, including CCSDT(Q) corrections; ΔE_{core} = core-correlation corrections at the cc-pCVTZ ROCCSD(T) level of theory; Δ_{ZPVE} = zero-point vibrational energy correction from cc-pV(5+d)Z ROCCSD(T) harmonic frequencies; Δ_{anharm} = anharmonic contribution to ZPVE from partial cc-pVTZ ROCCSD(T)VPT2 calculations; Δ_{rel} = scalar relativistic corrections [cc-pCV(T+d)Z ROCCSD(T)]; ΔDBOC = diagonal Born−Oppenheimer correction (aug-cc-pV(T+d)Z ROHF); Δ_{SOSE} = spin−orbit stabilization energy for $^2\Pi$ OH (ref 78). Final enthalpy of formation is relative to reference enthalpies given in Table 1.

Fundamental vibrational frequencies for *syn*-HOSO and *syn*-DOSO have been computed based on harmonic frequencies evaluated at the cc-pV(5+d)Z ROCCSD(T) level of theory, corrected for anharmonicity based on a cc-pV(T+d)Z ROCCSD(T) quartic force field. The resulting frequencies are in good agreement with results from rare gas trapping experiments,[27,28] especially considering the observed differences among Ar, Kr, and Xe matrix results. A previously tentative assignment[28] of a feature at 1050 cm^{-1} to the HOS bending mode has been confirmed.

A definitive enthalpy of formation for *syn*-HOSO has been provided based on the focal point approach,[47–50] along with reliable enthalpies for key reactions in the combustion of sulfur-containing fuels. The recommended (0 K) enthalpy of formation for *syn*-HOSO is −58.0 kcal mol^{-1}, while we recommend $\Delta_r H_{0K}°$= −38.6, 68.0, −64.4, and −80.1 kcal mol^{-1} for H + SO_2 → HOSO, HOSO → OH + SO, HOSO + H → H_2 + SO_2, and OH + HOSO → SO_2 + H_2O, respectively.

The present results represent the confluence of cutting edge computational methods paired with modern computer technology, which has enabled the definitive characterization of a seemingly simple radical species that is central to combustion of fossil fuels, yet has escaped accurate theoretical description in the previous decades.[26,29–44] The incorporation of the present thermochemical data into detailed kinetic models of combustion processes should enable more reliable predictions of the role of sulfur in the combustion of fossil fuels and the associated effects on NO_x chemistry in flames.

Acknowledgment. This research was supported by the U.S. Department of Energy, Office of Basic Energy Sciences, Combustion Program (Grant No. DE-FG02-00ER14748) and used resources of the National Energy Research Scientific Computing Center, which is supported by the Office of Science of the U.S. Department of Energy under Contract No. DE-AC02-05CH11231. S.E.W. would like to thank H. M. Jaeger and Dr. A. C. Simmonett for helpful discussions and B. E. Dye for assistance with some of the computations. Figures 1 and 2 were generated using HFSmol.[109]

References and Notes

(1) Hynes, A. J.; Wine, P. H. In *Gas Phase Combustion Chemistry*; Gardiner W. C., Jr., Ed.; Springer: New York, 1999.
(2) Cerru, F. G.; Kronenburg, A.; Lindstedt, R. P. *Proc. Combust. Inst.* **2005**, *30*, 1227.
(3) Blitz, M. A.; Hughes, K. J.; Pilling, M. J.; Robertson, S. H. *J. Phys. Chem. A* **2006**, *110*, 2996.
(4) The combustion chemistry of sulfur has recently been reviewed by Hynes and Wine (ref 1), while the work of Cerru et al. (ref 2) provides a concise summary of the issues in the modern combustion literature.
(5) Glarborg, P. *Proc. Combust. Inst.* **2007**, *31*, 77.
(6) Wheeler, R. *J. Phys. Chem.* **1968**, *72*, 3359.
(7) Halstead, C. J.; Jenkins, D. R. *Trans. Faraday Soc.* **1969**, *65*, 3013.
(8) Kallend, A. S. *Combust. Flame* **1969**, *13*, 324.
(9) Durie, R. A.; Johnsson, G. M.; Smith, M. Y. *Combust. Flame* **1971**, *17*, 197.
(10) Kallend, A. S. *Combust. Flame* **1972**, *19*, 227.
(11) Smith, O. I.; Wang, S.-N.; Tseregounix, S.; Westbrook, C. K. *Combust. Sci. Technol.* **1983**, *30*, 241.
(12) Webster, P.; Walsh, A. D. *Proc. Combust. Inst.* **1965**, *10*, 463.
(13) Zachariah, M. R.; Smith, O. I. *Combust. Flame* **1987**, *69*, 125.
(14) Kallend, A. S. *Trans. Faraday Soc.* **1967**, *63*, 2442.
(15) Drurie, R. A.; Johnson, G. M.; Smith, M. Y. *Combust. Flame* **1971**, *17*, 197.
(16) Cullis, C. F.; Mulcahy, M. F. R. *Combust. Flame* **1972**, *18*, 225.
(17) Glarborg, P.; Kubel, D.; Dam-Johansen, K.; Chiang, H.-M.; Bozzelli, J. W. *Int. J. Chem. Kinet.* **1996**, *28*, 773.

(18) Alzueta, M.; Bilbao, R.; Glarborg, P. *Combust. Flame* **2001**, *127*, 2234.
(19) Rasmussen, C. L.; Glarborg, P.; Marshall, P. *Proc. Combust. Inst.* **2007**, *31*, 339.
(20) Blitz, M. A.; McKee, K. W.; Pilling, M. J. *Proc. Combust. Inst.* **2000**, *28*, 2491.
(21) Hughes, K. J.; Blitz, M. A.; Pilling, M. J.; Robertson, S. H. *Proc. Combust. Inst.* **2002**, *29*, 2431.
(22) Dagaut, P.; Nicolle, A. *Proc. Combust. Inst.* **2005**, *30*, 1211.
(23) Dagaut, P.; Nicolle, A. *Int. J. Chem. Kinet.* **2005**, *37*, 406.
(24) Dagaut, P.; Lecomte, F.; Mieritz, J.; Glarborg, P. *Int. J. Chem. Kinet.* **2003**, *35*, 564.
(25) Dagaut, P.; Lecomte, F. *Fuel* **2003**, *82*, 1033.
(26) Frank, A. J.; Sadílek, M.; Ferrier, J. G.; Tureček, F. *J. Am. Chem. Soc.* **1996**, *118*, 11321.
(27) Isoniemi, E.; Khriachtchev, L.; Lundell, J.; Räsänen, M. *Phys. Chem. Chem. Phys.* **2002**, *4*, 1549.
(28) Isoniemi, E.; Khriachtchev, L.; Lundell, J.; Räsänen, M. *J. Mol. Struct.* **2001**, *563*−*564*, 261.
(29) Frank, A. J.; Sadílek, M.; Ferrier, J. G.; Tureček, F. *J. Am. Chem. Soc.* **1997**, *119*, 12343.
(30) Goumri, A.; Rocha, J.-D. R.; Laakso, D.; Smith, C. E.; Marshall, P. *J. Phys. Chem. A* **1999**, *103*, 11328.
(31) Boyd, R. J.; Gupta, A.; Langler, R. F.; Lownie, S. P.; Pincock, J. A. *Can. J. Chem.* **1980**, *58*, 331.
(32) Binns, D.; Marshall, P. *J. Chem. Phys.* **1991**, *95*, 4940.
(33) Laakso, D.; Smith, C. E.; Goumri, A.; Rocha, J.-D. R.; Marshall, P. *Chem. Phys. Lett.* **1994**, *227*, 377.
(34) Morris, V. R.; Jackson, W. M. *Chem. Phys. Lett.* **1994**, *223*, 445.
(35) Qi, J.-X.; Deng, W.-Q.; Han, K.-L.; He, G.-Z. *J. Chem. Soc., Faraday Trans.* **1997**, *93*, 25.
(36) Drozdova, Y.; Steudel, R.; Hertwig, R. H.; Koch, W.; Steiger, T. *J. Phys. Chem. A* **1998**, *102*, 990.
(37) McKee, M. L.; Wine, P. H. *J. Am. Chem. Soc.* **2001**, *123*, 2344.
(38) Wang, L.; Zhang, J. *J. Mol. Struct. (THEOCHEM)* **2002**, *581*, 129.
(39) Wang, B.; Hou, H. *Chem. Phys. Lett.* **2005**, *410*, 235.
(40) Napolion, B.; Watts, J. D. *Chem. Phys. Lett.* **2006**, *421*, 562.
(41) Ballester, M. Y.; Varandas, A. J. C. *Phys. Chem. Chem. Phys.* **2005**, *7*, 2305.
(42) Ballester, M. Y.; Varandas, A. J. C. *Chem. Phys. Lett.* **2006**, *433*, 279.
(43) Wierzejewska, M.; Olbert-Majkut, A. *J. Phys. Chem. A* **2007**, *111*, 2790.
(44) Wang, B.; Hou, H. *Chem. Phys. Lett.* **2005**, *410*, 235.
(45) Burcat, A. Ideal Gas Thermochemical Database. Available from ftp://ftp.technion.ac.il/pub/supported/aetdd/thermo-dynamics, 2002.
(46) Dunning, T. H., Jr.; Peterson, K. A.; Wilson, A. K. *J. Chem. Phys.* **2001**, *114*, 9244.
(47) East, A. L. L.; Allen, W. D. *J. Chem. Phys.* **1993**, *99*, 4638.
(48) Allen, W. D.; East, A. L. L.; Császár, A. G. In *Structures and Conformations of Non-Rigid Molecules*; Laane, J.; Dakkouri, M.; van der Veken, B.; Oberhammer, H., Eds.; Kluwer: Dordrecht, 1993.
(49) Császár, A. G.; Allen, W. D.; Schaefer, H. F. *J. Chem. Phys.* **1998**, *108*, 9751.
(50) Császár, A. G.; Tarczay, G.; Leininger, M. L.; Polyansky, O. L.; Allen, W. D. In *Spectroscopy from Space*; Demaison, J.; Sarka, K., Eds.; Kluwer: Dordrecht, 2001.
(51) Dunning, T. H., Jr. *J. Chem. Phys.* **1989**, *90*, 1007.
(52) Kendall, R. A.; Dunning, T. H., Jr.; Harrison, R. J. *J. Chem. Phys.* **1992**, *96*, 6796.
(53) Martin, J. M. L. *J. Chem. Phys.* **1998**, *108*, 2791.
(54) Martin, J. M. L.; Uzan, O. *Chem. Phys. Lett.* **1998**, *282*, 16.
(55) Bauschlicher, C. W., Jr.; Ricca, A. *J. Phys. Chem.* **1998**, *102*, 8044.
(56) Bauschlicher, C. W., Jr.; Partridge, H. *Chem. Phys. Lett.* **1995**, *240*, 533.
(57) Purvis, G. D.; Bartlett, R. J. *J. Chem. Phys.* **1982**, *76*, 1910.
(58) Scuseria, G. E.; Scheiner, A. C.; Lee, T. J.; Rice, J. E.; Schaefer, H. F. *J. Chem. Phys.* **1987**, *86*, 2881.
(59) Scuseria, G. E.; Janssen, C. L.; Schaefer, H. F. *J. Chem. Phys.* **1988**, *89*, 7382.
(60) Rittby, M.; Bartlett, R. J. *J. Phys. Chem.* **1988**, *92*, 3033.
(61) Raghavachari, K.; Trucks, G. W.; Pople, J. A.; Head-Gordon, M. *Chem. Phys. Lett.* **1989**, *157*, 479.
(62) Gauss, J.; Lauderdale, W. J.; Stanton, J. F.; Watts, J. D.; Bartlett, R. J. *Chem. Phys. Lett.* **1991**, *182*, 207.
(63) Bartlett, R. J.; Watts, J. D.; Kucharski, S. A.; Noga, J. *Chem. Phys. Lett.* **1990**, *167*, 609.
(64) Bartlett, R. J.; Watts, J. D.; Kucharski, S. A.; Noga, J. *Chem. Phys. Lett.* **1990**, *165*, 513.
(65) Noga, J.; Bartlett, R. J. *J. Chem. Phys.* **1987**, *86*, 7041.
(66) Noga, J.; Bartlett, R. J. *J. Chem. Phys.* **1988**, *89*, 3401.
(67) Watts, J. D.; Bartlett, R. J. *J. Chem. Phys.* **1990**, *93*, 6104.
(68) Scuseria, G. E.; Schaefer, H. F. *Chem. Phys. Lett.* **1988**, *152*, 382.
(69) Bomble, Y. J.; Stanton, J. F.; Kállay, M.; Gauss, J. *J. Chem. Phys.* **2005**, *123*, 054101.
(70) Kállay, M.; Gauss, J. *J. Chem. Phys.* **2005**, *123*, 214105.
(71) Stanton, J. F. *Chem. Phys. Lett.* **1997**, *281*, 130.
(72) Note that this method is different from the identically named connected-quadruple correction of: Kucharski, S. A.; Bartlett, R. J. *J. Chem. Phys.* **1998**, *108*, 9221.
(73) M RCC, a string-based quantum chemical program suite written by M. Kállay.
(74) Kállay, M.; Surján, P. R. *J. Chem. Phys.* **2001**, *115*, 2945.
(75) Stanton, J. F.; Gauss, J. Watts, J. D. Szalay, P. G.; Bartlett, R. J. with contributions from Auer, A. A.; Bernholdt, D. B; Christiansen, O.; Harding, M. E.; Heckert, M.; Heun, O; Huber, C.; Jonsson, D.; Jusélius, J.; Lauderdale, W. J.; Metzroth, T.; Michauk, C.; Ruud, K.; Schiffmann, F.; Tajti, A. and the integral packages: MOLECULE (Almlöf, J.; Taylor, P. R.), PROPS (Taylor, P. R.), and ABACUS (Helgaker, T.; Jensen, Aa.; Jørgensen, P.; Olsen, J.). See also: Stanton, J. F.; Gauss, J.; Watts, J. D.; Lauderdale, R. J.; Bartlett . See also: Stanton, J. F.; Gauss, J.; Watts, J. D.; Lauderdale, R. J.; Bartlett, *Int. J. Quantum Chem., Quantum Chem. Symp.* **1992**, *26*, 879. For current version see: http://www.aces2.de.
(76) Werner, H. J.; Knowles, P.; Lindh, R.; Manby, F. R.; Schütz, M.; Celani, P. ; Korona, T.; Rauhut, G.; Amos, R. D.; Bernhardsson, A; Berning, A.; Cooper, D. L.; Deegan, M. J. O.; Dobbyn, A. J.; Eckert, F.; Hampel, C.; Hetzer, G.; Lloyd, A. W.; McNicholas, S. J.; Meyer, W.; Mura, M. E.; Nicklass, A.; Palmieri, P. ; Pitzer, R.; Schumann, U.; Stoll, H.; Stone, R.; Tarroni, R.; Thorsteinsson, T. *MOLPRO*, version 2006.1, a package of ab initio programs.
(77) Karton, A.; Rabinovich, E.; Martin, J. M. L.; Ruscic, B. *J. Chem. Phys.* **2006**, *125*, 144108.
(78) Tajti, A.; Szalay, P. G.; Császár, A. G.; Kállay, M.; Gauss, J.; Valeev, E. F.; Flowers, B. A.; Vázquez, J.; Stanton, J. F. *J. Chem. Phys.* **2004**, *121*, 11599.
(79) Ruscic, B.; Pinzon, R. E.; Von Laszevski, G.; Kodeboyina, D.; Burcat, A.; Leahy, D.; Montoya, D.; Wagner, A. F. *J. Phys. Conf. Ser.* **2005**, *16*, 561.
(80) Ruscic, B. Active Thermochemical Tables In *2005 Yearbook of Science and Technology*, McGraw-Hill: New York, 2004; p 3.
(81) Ruscic, B.; Pinzon, R. E.; Morton, M. L.; von Laszevski, G.; Bittner, S. J.; Nijsure, S. G.; Amin, K. A.; Minkoff, M.; Wagner, A. F. *J. Phys. Chem. A* **2004**, *108*, 9979.
(82) In MOLPRO, this corresponds to what is described as RHF-UCCSD(T) theory.
(83) Knowles, P. J.; Andrews, J. S.; Amos, R. D.; Handy, N. C.; Pople, J. A. *Chem. Phys. Lett.* **1991**, *186*, 130.
(84) Lauderdale, W. J.; Stanton, J. F.; Gauss, J.; Watts, J. D.; Bartlett, R. J. *Chem. Phys. Lett.* **1991**, *187*, 21.
(85) Feller, D. *J. Chem. Phys.* **1993**, *98*, 7059.
(86) Helgaker, T.; Klopper, W.; Koch, H.; Noga, J. *J. Chem. Phys.* **1997**, *106*, 9639.
(87) Handy, N. C.; Yamaguchi, Y.; Schaefer, H. F. *J. Chem. Phys.* **1986**, *84*, 4481.
(88) Ioannou, A. G.; Amos, R. D.; Handy, N. C. *Chem. Phys. Lett.* **1996**, *251*, 52.
(89) Handy, N. C.; Lee, A. M. *Chem. Phys. Lett.* **1996**, *252*, 425.
(90) Kutzelnigg, W. *Mol. Phys.* **1997**, *90*, 909.
(91) Valeev, E. F.; Sherrill, C. D. *J. Chem. Phys.* **2003**, *118*, 3921.
(92) Perera, S. A.; Bartlett, R. J. *Chem. Phys. Lett.* **1993**, *216*, 606.
(93) Balasubramanian, K. *Relativistic Effects in Chemistry Part A Theory and Techniques*: Wiley: New York, 1997.
(94) Balasubramanian, K. *Relativistic Effects in Chemistry: Part B, Applications*, Wiley: New York, 1997.
(95) Cowan, R. D.; Griffin, D. C. *J. Opt. Soc. Am.* **1976**, *66*, 1010.
(96) Tarczay, G.; Császár, A. G.; Klopper, W.; Quiney, H. M. *Mol. Phys.* **2001**, *99*, 1769.
(97) These ROCCSD(T) computations utilized semicanonical orbitals, which will result in negligible deviations from analogous ROCCSD(T) computations in MOLPRO.
(98) Pedley, J. B. *Thermodynamic Data and Structures of Organic Compounds*; Thermodynamic Research Center: College Station, TX, 1994; Vol. 1.
(99) Nielsen, H. H. *Rev. Mod. Phys.* **1951**, *23*, 90.
(100) Watson, J. K. G. VPT2. In *Vibrational Spectra and Structure*; Durig, J. R. , Ed.; Elsevier: Amsterdam, 1977; p 1.
(101) INTDIF 2005 is a an abstract program written by Wesley D. Allen for Mathematica (Wolfram Research, Inc., Champagne, IL) to perform general numerical differentiation to high orders of electronic structure data.
(102) Decock, R. L.; McGuire, M. J.; Piecuch, P.; Allen, W. D.; Schaefer, H. F.; Kowalski, K.; Kucharski, S. A.; Musiał, M.; Bonner, A. R.; Spronk, S. A.; Lawson, D. B.; Laursen, S. L. *J. Phys. Chem. A* **2004**, *108*, 2893.

(103) INTDER 2005 is a general program written by W. D. Allen which performs various vibrational analyses and higher-order nonlinear transformations among force field representations.
(104) Allen, W. D.; Császár, A. G.; Szalay, P. G.; Mills, I. M. *Mol. Phys.* **1996**, *89*, 1213.
(105) Allen, W. D.; Császár, A. G. *J. Chem. Phys.* **1993**, *98*, 2983.
(106) Sarka, K.; Demaison, J. In *Computational Molecular Spectroscopy*; Jensen, P., Bunker, P. R. , Eds.; Wiley: Chichester, 2000; p 255.
(107) ANHARM is a FORTRAN program written for VPT2 analysis by Y. Yamaguchi and H. F. Schaefer, Center for Computational Quantum Chemistry, University of Georgia, Athens, GA, 30602, USA.
(108) Jacox, M. E. *Chem. Soc. Rev.* **2002**, *31*, 108.
(109) Wheeler, S. E. *HFSmol*; University of Georgia: Athens, GA, 2008.

JP9029387